The Relationship Between Rat Intestinal Permeability and Hydrophilic Probe Size

Majella E. Lane,[1] Caitriona M. O'Driscoll,[1] and Owen I. Corrigan[1,2]

Received May 17, 1996; accepted July 1, 1996

Purpose. The relationship between rat intestinal permeability (P_{app}) of a range of hydrophilic probe molecules and probe geometry was examined.

Methods. Molecules studied included mannitol, the polyethylene glycols (PEGs) 400, 900, and 4000, the dextran conjugated dye Texas Red® (MW 3000) and the polysaccharide inulin (MW 5500). Molecular surface area, volume and cross-sectional diameter for each probe were determined from computer models. The effect of the bile salt sodium cholate, and bile salt: fatty acid mixed micelles on probe intestinal permeability was also studied.

Results. Of the size parameters tested, cross-sectional diameter correlated best with log intestinal permeability. The data was fitted to a relationship of the form $P_{app} = P^0_{app} \exp(-Kr_{ca})$ where r_{ca} is the molecular cross sectional radius, P^0_{app} and K are constants. Estimates of equivalent pore radii (R) were also made; the use of r_{ca} giving the most reasonable estimate of R. Absorption of all probes was enhanced by both simple and mixed micellar systems.

Conclusions. For large hydrophilic probes, and possibly protein drugs, cross sectional diameter is a more important size parameter than volume based values for evaluating size-related retarded absorption. The relationship established may be used as a tool to assess absorption enhancement potential of excipients.

KEY WORDS: rat intestinal permeability; hydrophilic probe molecules; probe geometry; bile salt: fatty acid micelles.

INTRODUCTION

Passive absorption of soluble drugs across the intestine is generally considered to involve intracellular and paracellular pathways. Furthermore, M-cells or Peyer's patches have been implicated in the absorption of nano- and micro-particulates (1). With the growth of pharmaceutical biotechnology resulting in an increasing number of polypeptide based drugs, there is increased interest in quantifying absorption of hydrophilic macromolecular drugs. Absorption of hydrophilic solutes is considered to be restricted to the paracellular route i.e. through tight junctions between cells (2,3). Equivalent pore radii have been estimated based on the equations of Renkin and Solomon (4,5). Previously it was assumed that absorption of large hydrophilic probes was inversely proportional to molecular weight (6). A linear relationship between absorption and cross-sectional diameter for probes in the narrow range 164–400 daltons has also been reported (7).

In this work a range of unionised hydrophilic 'probe' molecules, with a wider molecular weight range and varying geometries, was used to study intestinal permeability. Probe molecules studied included mannitol, the polyethylene glycols (PEGs) 400, 900 and 4000, the polysaccharide inulin and a dextran dye, Texas Red®. Molecular modelling programmes were used to examine probe geometry in a simulated water environment. The effects of sodium cholate, and sodium cholate: linoleic acid micellar systems, on the relationship between intestinal permeability and molecular size were also examined.

The apparent permeability coefficient (P_{app}) was determined from the solute fraction remaining in the intestinal lumen of length, 1, C(1)/C(0) using equation 1:

$$P_{app} = -(Q/2\pi rl).\ln(C(1)/C(0)) \quad (1)$$

where Q is the flow rate (ml s^{-1}) and r is the effective lumenal radius (8). If membrane transport of hydrophilic solutes is restricted to the aqueous pore route then the permeability coefficient may be described (9) as:

$$P_{app} \sim P_{paracell} = \varepsilon.D.F(r/R)/\delta \quad (2a)$$

where ε is the porosity or volume fraction of aqueous pores, F(r/R) is a diffusional hindrance factor and δ is the pore length. For a given porous membrane under constant experimental conditions:

$$P_{app} = m.D.F(r/R) \quad (2b)$$

where m is a constant.

MATERIALS AND METHODS

Materials

^{14}C-PEG 4000 (molecular weight distribution 3600–4000, Amersham Technical Data Sheet) and ^{3}H-Inulin, were obtained from Amersham International, UK and ^{3}H-PEG 900 (molecular weight distribution 800–1000, NEN Batch Data Sheet) from New England Nuclear. PEG 4000, inulin, mannitol, sodium cholate and linoleic acid were obtained from Sigma, St. Louis, PEG 400 (molecular weight distribution 380–420, Aldrich Technical Data Sheet) from Aldrich, UK and Texas Red® from Molecular Probes, Oregon.

Solutions

Final concentrations of probe solutions were as follows; 1% w/v for all PEG solutions, 0.5% w/v mannitol, 0.01% w/v Texas Red and 0.1% w/v inulin. Solutions were prepared in Sorensons phosphate buffer pH 7.4. Simple micelle solutions consisted of 40 mM sodium cholate and mixed micellar solutions of 40 mM sodium cholate: 40 mM linoleic acid. Osmolarity was adjusted using sodium chloride to 295–300 mOsm/kg of H_2O, measured using an Osmometer (Fiske Associates, Massachusetts).

Rat Intestinal Perfusion Model

A rat gut perfusion model was used to estimate intestinal permeability (8). Male Sprague-Dawley rats of mean weight 250g were used. Animals were fasted overnight and anaesthetised using pentobarbital sodium. The intestinal perfusion rate was 0.2 ml min^{-1} and the upper small intestinal length 33.3

[1] University of Dublin, Department of Pharmaceutics, Trinity College, Dublin 2, Ireland.
[2] To whom correspondence should be addressed.

0724-8741/96/1000-1554$09.50/0

cm. Samples were collected at 10-minute intervals for 2 hours. Blood was taken from the jugular vein and either analysed directly or, centrifuged at 2800 rpm for 10 minutes for plasma analysis.

Analysis

^{14}C-PEG 4000, ^{3}H-PEG 900, and ^{3}H-Inulin were analysed by liquid scintillation counting in a Packard® TriCarb 2500TR liquid scintillation analyzer. Quench correction was carried out by the method of external standardisation.

A spectrophotometric assay for mannitol was employed based on the conversion of mannitol to fructose by the enzyme mannitol dehydrogenase (10). Samples were assayed at 340 nm in a Hewlett-Packard UV-Vis spectrophotometer.

High-performance liquid chromatography was used to assay PEG 400 after post-column derivatisation (11). A Shimadzu A412 spectrofluorimeter was used to analyse the Texas Red® probe with λ_{em} = 590 nm and λ_{ex} = 612 nm.

Molecular Modelling

Molecular modelling studies were carried out by building structures in Hyperchem® (Autodesk, Inc.) and importing the co-ordinates into Chem-X® (Chemical Design Limited). Subsequently geometric manipulations including rotation, translation and geometry calculations such as bond lengths, nonbonded distances and bond angles were performed. The molecular probes were modelled using Molecular Mechanics (MM) force fields. Solvent effects were mimicked by adjusting dielectric constants and performing simulated annealing.

Relationships between variables were tested using the nonlinear curve fitting and model development program Minsq 4 (Micromath Inc.). Model suitability was assessed using the Model Selection Criterion (MSC).

RESULTS AND DISCUSSION

Intestinal Permeability and Probe Size

The P_{app} of the molecular probes in buffer tended to decrease with increasing molecular weight (Table 1), though not in rank order. Thus, in the case of mannitol and PEG 400 the lower molecular weight probes, the P_{app} of PEG 400 was greater than that of the lower molecular weight mannitol. The absorption of the large probes, PEG 4000 and inulin, is consistent with previous reports (2,3). To confirm systemic absorption plasma concentrations were determined after the two hour perfusion period for the probes with the exception of Texas Red. A similar inverse trend was seen between molecular size and blood levels (Table 2).

Geometric parameters including cross-sectional diameters, surface areas and volumes were calculated from computer models of each probe. Hollander et al. (7) have reported similar values of cross-sectional diameter for mannitol and PEG 400 (Table 1). These workers also suggested that PEG polymers fold above 12 to 14 monomer units which is supported by the computer generated models for PEG 900 and PEG 4000 (Figure 1).

Correlations of Probe Size and P_{app}

The relationships between the size properties; molecular weight, cross sectional diameter, area, volume and P_{app} were examined. The best linear relationship ($y = -0.432x - 8.814$, $r^2 = 0.98$) was obtained when ln P_{app} was plotted against cross-sectional diameter (Figure 2). PEG samples are not monodisperse. The P_{app} values for these samples however, do not deviate significantly from the trend line. Furthermore computer models of the molecular weight extremes indicate that the cross sectional diameter varies by less than 2% over the range for PEG 4000 and by less than 1% for PEG 900.

The data in Figure 2 and Table 1 indicate an empirical relationship of the form:

$$P_{app} = P^{0}_{app} \exp(-K.r_{ca}) \quad (3)$$

The parameter P^{0}_{app} may be considered as the intrinsic pore permeability, i.e. the P_{app} in the absence of any size-related hindrance to pore transport and K is a hindrance intensity factor, the larger K the more sensitive is the membrane permeability to probe size. The value of K obtained indicates that in the absence of enhancers, P_{app} will decrease by 50% for every 0.8 Å increase in r_{ca}. Thus the relationship indicates that, indeed, very large molecules may be absorbed, but at exponentially declining rates. The exponential relationship may arise from a broad size distribution of pores and/or a time dependent fluctuation in pore sizes. It has been suggested that changes in perme-

Table 1. Experimental Permeability Coefficients (P_{app}) of Molecular Probes from Buffer, Bile Salt (40 mM), and Mixed Bile Salt:Fatty Acid (40:40 mM) Micellar Systems

Probe	Cross-sectional Diameter (Å)	P_{app} cm/sec × 10^6 ± S.E.		
		Buffer	Sodium Cholate (40 mM)	Sodium Cholate /Linoleic Acid (40:40 mM)
Mannitol	6.3	8.2 ± 0.50	45.8 ± 1.50	32.90 ± 5.6
PEG 400	5.6	16.0 ± 1.80	41.9 ± 3.20	31.10 ± 2.2
PEG 900	8.3	4.3 ± 0.07	11.3 ± 4.00	14.60 ± 1.7
Texas Red	10.1	2.1 ± 0.17	6.0 ± 2.00	8.27 ± 2.4
PEG 4000	12.0	0.6 ± 0.09	2.0 ± 0.14	3.40 ± 0.5
Inulin	14.8	0.3 ± 0.07	1.5 ± 0.80	2.00 ± 0.8

Table 2. Blood Levels of Molecular Probes Following Perfusion for 120 Mins in Buffer, Sodium Cholate (NaC), 40 mM, and Mixed Micelles of NaC and Linoleic Acid (L.A.) 40:40 mM

Molecular Probe	Blood Level mg ml^{-1} × 10^2 ± S.E.		
	Control	NaC 40 mM	NaC:L.A. 40:40 mM
Mannitol	8.9 ± 1.20	20.4 ± 3.60	21 ± 2.00
PEG 400	39.0 ± 6.00	81.0 ± 12.60	50 ± 8.30
PEG 900	1.7 ± 0.36	2.50 ± 0.55	5.9 ± 0.82
PEG 4000	0.9 ± 0.20	2.75 ± 0.68	3.38 ± 0.92
Inulin	0.05 ± 0.01	0.22 ± 0.06	0.693 ± 0.10

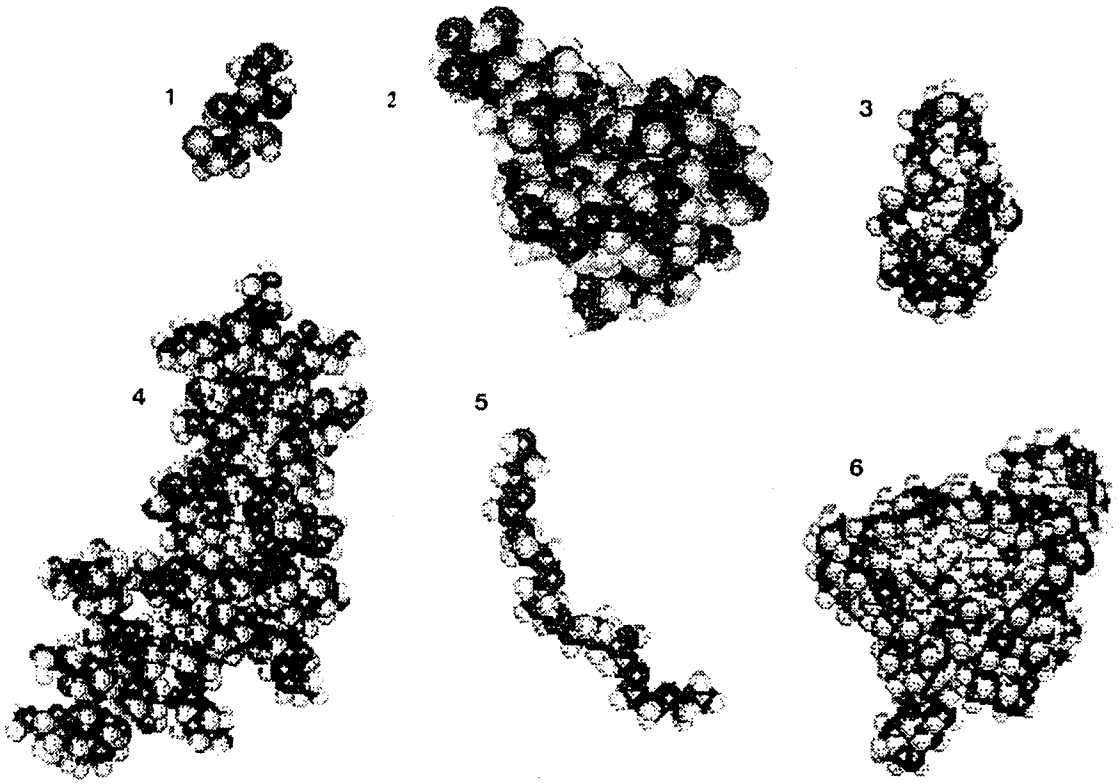

Fig. 1. Computer generated models of the hydrophilic probe molecules, (1) mannitol, (2) Texas Red, (3) PEG 900, (4) Inulin, (5) PEG 400 (6) PEG 4000.

ability may be due to changes in the frequency of "opened" versus "closed" pores (12). Madara et al. (13) suggested that such permeability changes may be caused by an altered conformation of a few existing pores without substantial changes in their cross-sectional area.

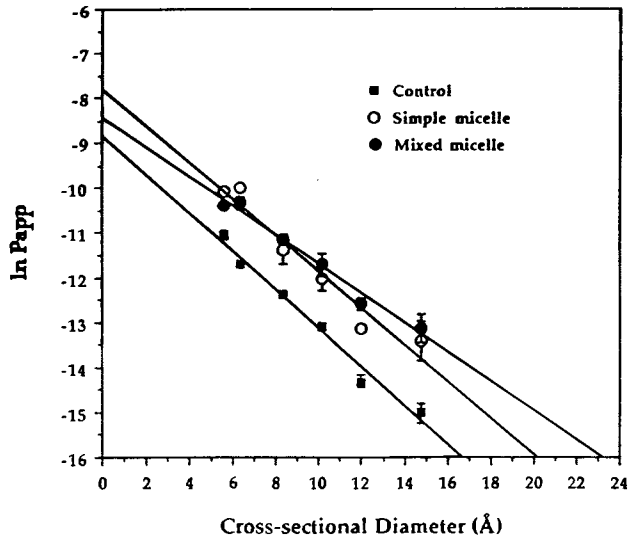

Fig. 2. Relationship between ln P_{app} of the molecular probes, from buffer, simple bile salt micelles (40 mM) and mixed bile salt: fatty acid (40: 40 mM) micellar systems, and cross-sectional diameter of the probes.

Equivalent Pore Radii

Transport data for small hydrophilic probes has been used to determine an equivalent pore radius assuming that tight junctions can be described by a set of uniform pore channels (14).

Renkin has described the dimensionless molecular restriction function F(r/R), for spherical solutes diffusing within a cylindrical channel (4) as:

$$F(r/R) = (1 - r/R)^2[1 - 2.104(r/R) + 2.09(r/R)^3 - 0.95(r/R)^5] \quad (4)$$

which compares molecular radius, r, with pore radius, R, and where $0 < F(r/R) < 1.0$. This Renkin filtration factor is a polynomial function which approaches zero as the molecular radius approaches the pore radius. Theoretically, equation 4 is applicable when $r/R \leq 0.4$ and it has been used to describe permeability via the aqueous pores in the intestine (9).

For any pair of probes of radii r and r_x:

$$r_x.P_x/r.P = F(r_x/R)/F(r/R) \quad (5)$$

Since the permeability coefficients (P_x, P) and the molecular radii are known, the effective pore radius, R, may be calculated by successive approximation (9). In this manner, the unknown parameters in Equation 2 cancel.

Since the best correlation was obtained using cross-sectional diameter rather than molecular volume (Figure 2, Table 1) the former values were used to calculate the pore radius by successive approximation. When the three smaller probes,

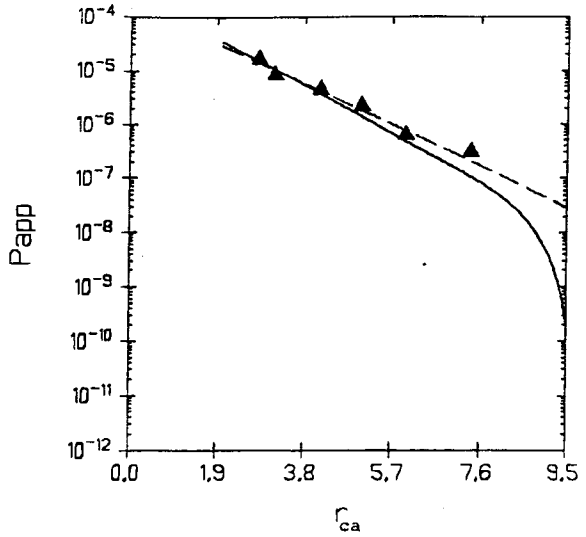

Fig. 3. The paracellular permeability coeffients of the molecular probes versus their cross-sectional radius. The solid line depicts the best fit to equations 2 and 4 assuming a pore radius of 9.20 Å.

mannitol, PEG 400 and PEG 900, were used (i.e. those for which r/R $</\simeq$ 0.4) an average pore radius of 9.20 Å ± 3.7 S.D., was obtained. Using the same method of calculation and probes of similar dimensions Adson et al. (9) reported a mean pore radius of 12.0 Å ± 1.9 S.D. for Caco-2 cells. In the current work when data from all probes were used the mean pore radius estimate was 12.06 Å ± 5.27 S.D. which reflects the fact that for the larger probes r/R greatly exceeded 0.4.

Alternatively the pore radius was estimated by non-linear least squares fitting of the experimental permeability data and equations 2 and 4. Using this method and the three smaller probes an average pore radius of 8.33 Å ± 3.12 S.D. was obtained, a similar value of 9.55 Å ± 1.73 S.D. was estimated when all six probes were used. The estimate determined using the cross-sectional radii of small sized probes is consistent with the reported radius of 6.2 Å for rat jejunum (15).

The permeability coefficients of the probes were plotted in semi-log format against the molecular radii and the data was fitted using equations 2 and 4, assuming a pore radius of 9.2 Å (Figure 3), together with the prediction of equation 3. It is evident that significant divergence between the two models occurs at large molecular sizes, the P_{app} decreasing sharply towards zero when the Renkin function prediction is used, a trend not evident in the data. Equation 3 also gave the better correlation coefficient and MSC.

Effects of Enhancers on Pore Permeability

The addition of sodium cholate significantly ($p < 0.05$) enhanced the P_{app} of all the probes relative to the control. Enhancements were also observed in the presence of the sodium cholate: linoleic acid mixed micellar system (Table 1). The extent of the relative enhancements obtained with the two micellar systems differed depending on the probe size. The simple micellar system enhanced the P_{app} of the lower molecular weight probes (up to 400) to a greater degree compared to the mixed micellar system. In contrast, greater relative enhancements for the larger probes (>400) were observed with the mixed micellar system. In the case of both micellar systems the P_{app} decreased as the molecular weight increased (Table 1). The blood levels for the probes in the presence of the enhancers are also listed in Table 2 and are qualitatively consistent with enhanced absorption.

The permeability coefficient and probe size data were fitted to equation 3. Cross-sectional diameter again gave the best correlation for both enhancer systems. The fit to the sodium cholate data was poorest. The parameter estimates are compared to those obtained in the absence of enhancer in Table 3 and the semilog plots are shown in Figure 2. In the presence of both simple and mixed micellar systems an upwards shift in the linear relationship is evident. An increase in P^0_{app} in the presence of enhancers suggests an effect on ε, D or δ, (Equation 2a). More data will be necessary to clarify the situation.

The increases in probe permeabilities in the presence of both simple and mixed micellar systems were also used to estimate equivalent pore radii in the presence of the enhancers. Using the non linear least squares method and all six probes the pore radius estimate increased to 11.776 Å ± 2.76 S.D. in experiments with simple micelles and to 16.736 Å ± 4.35 S.D. for those with the mixed micellar system. Therefore this approach to the analysis of the data suggests that the presence of the enhancers caused between a 1.2 to 1.8 fold increase in effective pore radius as compared to the control. A problem with this form of analysis is (in contrast to Equation 3) the assumption that despite an increase in pore area the volume fraction of aqueous pores remains unchanged. The slopes of the lines relating permeability coefficient to cross-sectional diameter are significantly different for the control and mixed micellar systems ($p < 0.05$). The significant difference in intercept between the simple micellar system and control is consistent with an increase in ε, the volume fraction of aqueous pores.

Table 3. The Effects of Simple Bile Salt Sodium Cholate (NaC) (40 mM) and Mixed NaC : Linoleic Acid (40:40 mM) Micellar Systems on the Relationship Between ln $P_{paracell}$ and Cross-Sectional Diameter of the Probe Molecules

System	P^0_{app} cm/sec ± S.E. ($\times 10^5$)	K ± S.E.	r^2	0.693/K
Control	15.36 ± 7.11	0.432 ± 0.087	0.981	1.6
Sodium Cholate (NaC) 40 mM	42.18 ± 3.62	0.401 ± 0.039	0.935	1.7
NaC : Linoleic Acid 40:40 mM	22.25 ± 8.37	0.325 ± 0.042	0.982	2.1

REFERENCES

1. J. Kreuter, *Adv. Drug Del. Rev.* **7**:71–86 (1991).
2. J. R. Pappenheimer and K. R. Reiss, *J. Membr. Biol.* **100**:123–136 (1987).
3. T. Y. Ma, D. Hollander, R. A. Erickson, H. Truong and P. Krugliak, *Am J. Physiol.* **260**:G669–G676 (1991).
4. F. E. Curry. In E. M. Renkin and C. C. Michel (eds.), Handbook of Physiology, Section 2, The Cardovascular System, Vol. IV, Microcirculation. Am. Physiol. Soc., Bethsada, MD, 1984, pp. 309–374.
5. A. K. Solomon, *J. Gen. Physiol.* **51**:335s–364s (1968).
6. V. S. Chadwick, S. F. Phillips and A. F. Hoffman, *Gastroenterol.* **73**:241–246 (1977).
7. D. Hollander, D. Ricketts and C. A. R. Boyd, *Can. J. Gastroenterol.* **2** (suppl. A):35A–38A (1988).
8. I. Komiya, K. Y. Park, A. Kamani, N. F. H. Ho and W. I. Higuchi, *Int. J. Pharm.* **4**:249–262 (1980).
9. A. Adson, T. J. Raub, P. S. Burton, C. L. Barsuhn, A. R. Hilgers, K. L. Audus and N. F. H. Ho, *J. Pharm. Sci.* **83**:1529–1535 (1994).
10. P. G. Lunn, C. A. Northrop and A. J. Northrop, *Clin. Chim. Acta* **183**:163–170 (1989).
11. I. M. Kinahan and M. R. Smyth, *J. Chromatog.* **565**:297–307 (1991).
12. M. Cereijido. In M. Cereijido (ed.), *Tight Junctions*, CRC Press, Boca Raton, FL, 1993, pp. 1–13.
13. J. L. Madara, D. Barenberg and S. Carlson, *J. Cell Biol.* **102**:2125–2136 (1986).
14. K. H. Soergel, *Gastroenterol.* **105**:1247–1250 (1993).
15. N. F. H. Ho, J. Y. Park, P. F. Ni, and W. I. Higuchi, In W. Crouthamel and A. C. Sarapu (eds.), *Animal Models for Oral Drug Delivery in Man*, Am. Pharm. Assoc. Washington, D.C. 1983, pp. 27–106.